Communication in Implantable Medical Devices: FEM Simulation to Evaluate the Coating Effects on Transmission

Antonio Coviello*
DEIB Politecnico di Milano
Milan, Italy
antonio.coviello@polimi.it

Letizia Mangiagalli*
DEIB Politecnico di Milano
Milan, Italy
letizia.mangiagalli@mail.polimi.it

Maurizio Magarini
DEIB Politecnico di Milano
Milan, Italy
maurizio.magarini@.polimi.it

*Both authors contributed equally to this research

***Abstract* — Implantable medical devices hold great promise for treating nervous system disorders. However, their small size requires communication with an external device to process electrophysiological signals. The transmission of these signals is often hindered by biocompatible encapsulation materials and surrounding biological tissues. This study uses FEM simulations in COMSOL Multiphysics to assess how the device's coating and biological tissues affect 2.4 GHz data transmission, a frequency within the ISM band for implantable device communications.. A compact Planar Inverted-F Antenna (PIFA) is used, and S11/S22 parameters are calculated to assess transmission efficiency. Since the coating layer hinders transmission depending on its thickness and material properties, simulations were conducted using three different body types representing varying Body Mass Index (BMI) levels to account for inter-patient variability. Implant safety was evaluated by calculating the Specific Absorption Rate (SAR) and the local temperature increase. The results presented in this work serve as a pilot study to assess the effects of encapsulation materials on wireless communication in implantable devices, laying the groundwork for future *ex vivo* and *in vivo* research.**

***Keywords*— Wireless data transmission, finite element method simulation, implanted electronic devices, preclinical study.**

I. Introduction

Some neurological conditions, like peripheral neuropathies, can disrupt nerve signal transmission, severely impairing motor and sensory functions. These disorders may arise from systemic diseases like diabetes mellitus, metabolic imbalances such as hyperthyroidism, nutritional deficiencies, or exposure to toxic substances [1]. In cases where the neuropathy is not associated with systemic causes, restoring nerve function remains a major clinical challenge.

Traditional treatments for neuropathies typically involve surgical interventions, such as autologous nerve grafting or microsurgical repair. However, the scarcity of healthy donor nerves and their limited effectiveness significantly constrain these approaches [2]. In response to these limitations, novel strategies have emerged, most notably the development of implantable devices, which offer a promising avenue for improving outcomes in patients with peripheral neuropathies [3]. These technologies are essential to modern healthcare, improving both quality of life and life expectancy for affected individuals. However, notable challenges remain, especially in designing biocompatible devices that can relaible communicate with the external environment. A critical factor is represented by the encapsulation material. If not properly designed, the coating may hinder the implant's wireless communication.

Despite advances in implantable systems, no comprehensive study has defined the optimal encapsulation conditions required for effective communication. Furthermore, due to inter-subject variability in physiological properties, a personalized approach that accounts for individual patient characteristics is crucial to ensure broad applicability. Our study addresses this gap through a detailed, simulation-based investigation aimed at identifying optimal antenna encapsulation configurations.

The considered antenna is a Planar Inverted-F Antenna (PIFA), which is widely used in implantable wireless applications due to its compact design and stable performance. A study by Khabiri *et al.* [4] reported its implementation at 402 MHz, demonstrating excellent transmission efficiency (S11 of -28 dB) and compliance with safety limits for the Specific Absorption Rate (SAR). However, the study in [4] did not include any encapsulation material for biocompatibility, which, as our simulations reveal, plays a significant role in increasing the scattering parameters.

Our results show that polydimethylsiloxane (PDMS), a flexible and biocompatible polymer commonly used for encapsulation, causes substantial signal attenuation. To address this, we refer to solutions proposed in other studies, where rigid ceramic substrates were used without polymeric coatings [5, 6], achieving favorable S11 values (< -10 dB). Despite their performance, these rigid designs are associated with a higher risk of adverse tissue reactions. This highlights the importance of optimizing polymeric encapsulation strategies, including the use of nanocomposite materials, to balance mechanical compatibility and signal transmission. Our operating frequency is near 2.4 GHz, which falls within the Industrial, Scientific, and Medical (ISM) band used by many low-power wireless systems. Although this study does not implement a full Bluetooth Low Energy (BLE) communication protocol, the electromagnetic analysis focuses on the antenna's performance under conditions relevant to such applications.

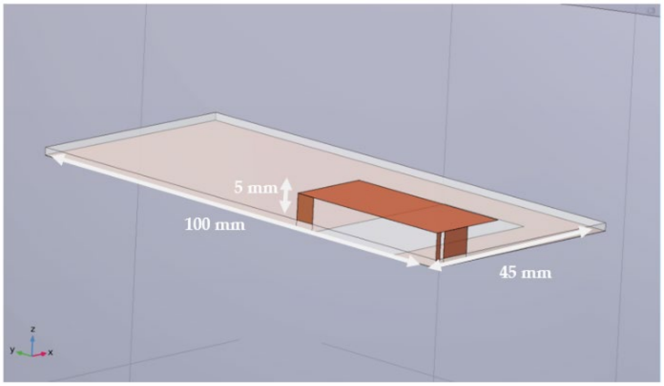

Figure 1. Antenna PIFA's COMSOL geometry.

The contributions of this work are threefold. First, we introduce a personalized modeling framework that accounts for different body compositions across a range of Body Mass Index (BMI) values, reflecting individual physiological characteristics and enhancing the relevance of the findings. Second, we incorporate a temporal evaluation of implant behavior by simulating the formation of a fibrotic capsule, thereby assessing long-term effects on transmission performance. Third, we examine the translatability of human-based results to preclinical animal models by evaluating a rat tissue model, in order to determine how well these models can predict human outcomes.

The rest of the paper is organized as follows. The antenna design is introduced in Sec. II. Section III describes the FEM simulation framework, including the definition of performance metrics and key parameters. Section IV presents the numerical results. Finally, conclusions are drawn in Sec. V.

II. Design of the Antenna

A key challenge in the design of implantable devices is ensuring that the encapsulation material is both biocompatible and mechanically compatible with surrounding tissues. Materials that are significantly stiffer than soft tissues can induce stress at the interface, potentially triggering chronic inflammation and leading to implant failure. PDMS, a widely used polymer in biomedical applications, is particularly suitable for subcutaneous implantation due to its flexibility, low hardness, and elastic modulus comparable to that of human skin [7]. Its properties, such as chemical resistance, thermal dissipation, and optical transparency, further support its use in wireless implantable systems, where reliable operation and protection of internal components are essential [8].

A common biological response to implanted materials is the formation of a fibrotic capsule, which can electrically isolate the device and reduce its effectiveness [9]. This phenomenon is influenced by the mechanical and chemical characteristics of the coating, reinforcing the need to tailor materials that reduce mechanical mismatch and tissue response. To enhance long-term compatibility, flexible polymeric coatings are used, as they accommodate tissue deformation and minimize the risk of delamination or fluid infiltration, either of which could compromise device integrity [8]. Additionally, incorporating nanocomposites like graphene into these polymers may improve both mechanical robustness and electrical performance [10].

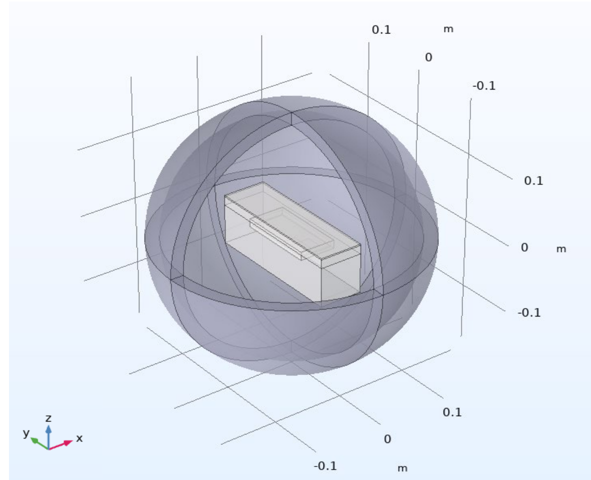

Figure 2. Antenna inserted into the biological tissue model with fibrotic capsule.

Recent studies have also investigated how the encapsulation affects wireless signal transmission. In particular, interfacial layers between the device and surrounding tissues can attenuate the signal, which must be considered during design. This is especially critical for implants operating in the 2.4 GHz ISM band, a commonly used frequency range that offers sufficient bandwidth and penetration for medical telemetry. Unlike ultrasonic or galvanic alternatives, which suffer from strong attenuation or limited data throughput in deep tissue, RF-based communication at this frequency is more suitable for continuous, low-power data exchange [11, 12].

Different types of antennas can be used for implantable applications, each offering advantages in size, efficiency, and integration. Two examples are U-shaped and spiral antennas [13, 14]. PIFA antennas are well-suited for body-implanted systems due to their compact dimensions, stable impedance, and effective radiation efficiency near biological tissues [15]. They are also widely used in commercial electronics and wireless body sensor networks for their ease of integration and low production costs [16].

In our simulations, we used the PIFA antenna shown in Fig. 1, which is tuned to operate between 2.1 and 2.9 GHz, thus covering the 2.4 GHz band commonly used for medical wireless communication. This frequency suits telemetry and implantable device constraints. To mitigate signal attenuation from tissue absorption, strategies such as geometrical optimization and insulating materials have been proposed [17]. For instance, a study found that a 4 mm Zirconia layer reduced signal loss compared to other materials [18]. Dielectric coatings like Teflon, ceramics, Zirconia, PEEK, and Silastic can enhance biocompatibility and signal efficiency [17]. The material and thickness of the encapsulation are crucial for antenna power and performance [18].

III. FEM Simulation with COMSOL

To evaluate the influence of encapsulation materials and biological tissues on signal transmission, an FEM simulation was conducted using COMSOL Multiphysics (version 6.2) [19].

The simulation domain included a spherical layer surrounding the antenna, representing the far field, which absorbs outgoing electromagnetic waves and prevents reflection artifacts (Fig. 2). The antenna was first simulated in free space to establish a reference. Then, it was encapsulated with PDMS layers of varying thicknesses: 0.5 mm, 1 mm, and 2 mm, to assess the impact of the coating.

To further investigate the effect of advanced materials, an additional simulation was performed with a nanocomposite layer composed of PDMS and graphene, following insights from previous studies that demonstrated improved electromagnetic behavior with such configurations [10]. A biological tissue model based on data available in [20] was implemented, composed of three primary layers: muscle (6 cm thick), skin (2 mm thick), and fat, whose thickness varies according to body mass index (BMI). A fibrotic capsule (0.5 mm thick) was also included to account for chronic biological responses.

The complete structure, comprising the antenna, graphene layer (G), PDMS, fibrotic capsule, and biological tissues, is illustrated in Fig. 3. To introduce inter-patient variability, simulations were conducted across three BMI categories: underweight, normal weight, and overweight, using World Health Organization (WHO) classification guidelines. Unlike skin [21] and muscle [22], fat thickness is directly correlated with BMI. The study in [23] proposed the following linear relationship to describe this:

$$BMI = 16.99 + 0.38 \cdot t_f \qquad (1)$$

where t_f is the subcutaneous fat thickness in mm. Using this equation, fat layer thicknesses were calculated for BMI values of 17.5, 22, and 27, resulting in 2 mm, 12.8 mm, and 25.6 mm, respectively. Finally, to explore the translational relevance of the model, an additional simulation was carried out using a rat tissue model. The layered structure included fibrotic capsule, muscle, fat, and skin, with physical and electrical properties derived from literature sources, enabling a direct theoretical comparison between human and preclinical scenarios.

A. Evaluation metrics

Several parameters were used to quantify the performance of the PIFA antenna studied. When the signal is transmitted from the implanted device to the external unit and vice versa, the radio waves experience reflection at the interface between materials with different properties, particularly permittivity, magnetic permeability, and electrical conductivity. To quantify this phenomenon, the scattering parameters S11 (input reflection coefficient) and S22 (output reflection coefficient) were calculated. These parameters, measured in decibels, represent the fraction of wave power reflected at the antenna input and output, respectively [24]. To minimize power reflection at the input and output, the values of S11 and S22 should be a negative value in dB as low as possible. The value of -10 dB can be chosen as a threshold for this purpose, as it defines an acceptable value for the scattering parameters in these applications, as also noted in [5]. Although S21 is commonly used in multi-port systems to assess transmission between antennas, it is not applicable in our single-antenna, in-body simulation setup. In implantable contexts, S11 and S22 are more relevant for evaluating the interface losses and radiation efficiency, which directly influence the reliability of external communication.

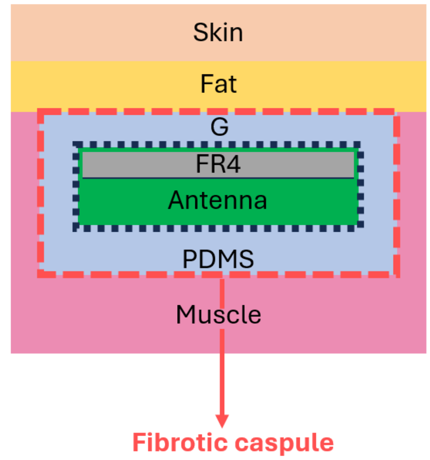

Figure 3. Tissue model including in order: skin, fat, muscle, fibrotic capsule, PDMS + nanocomposite coating (G), and the PIFA antenna with its substrate in FR4.

Another considered parameter was the SAR (W/kg), which measures the absorption of electromagnetic energy by tissues. It is given by

$$\mathrm{SAR} = \frac{\sigma \cdot |E|^2}{\rho}, \qquad (2)$$

where σ is the electrical conductivity of the tissues [S/m], E is the electric field [N/C], and ρ is the density of the tissue [kg/m^3]. Depending on the application, exposure time and installation site, there are different tolerance levels indicated by the Federal Communications Commission [17, 25]. For this application, a SAR cutoff value of 1.6 (W/kg) was arbitrarily selected as an average over 1 g of tissue (not 10 g because we are dealing with small masses of tissue), following the most restrictive guidelines indicated. The *temperature* is indicated as the last parameter [25].

The last evaluated parameter was the thermal impact of the implanted antenna, which was assessed by determining the steady-state temperature rise, as follows:

$$Q = c_m \cdot (T_h - T_c), \qquad (3)$$

where Q is the heat emitted per unit volume [W/ m^3], c_m is the specific heat of the tissue [J·kg/m^3], T_h [K] is the highest temperature in the system (due to the presence of antenna, which is unknown in this case), and T_c [K] is the lowest temperature in the system (corresponding to 37° C, i.e. body temperature).

B. Simulation parameters

The integration of various materials into the simulation required defining specific properties for each material (magnetic permeability, dielectric constant, electrical conductivity, density, and thermal conductivity). Some properties were preloaded into COMSOL, while others were taken from the literature. Tables 1, 2, and 3 show the electrical properties used in the simulations for the antenna materials and for human and rat biological tissues, respectively. Table 4 presents the thermal parameters of the tissues. It is important to note that the electromagnetic and thermal field values used in the simulation are approximated as constant over both space and time. This assumption simplifies the model while allowing meaningful evaluation of antenna performance and tissue interactions.

Table 1 Electrical properties of antenna materials.

Material	Dielectric constant (permittivity) [C2/(N·m^2)]	Permeability [H/m]	Electric Conductivity [S/m]
Air	1	1	0
Copper	1	1	5.998e7
FR4	4.4	1	0
PDMS	2.8	1	5e-13
PTFE	2.02	1	0
Ferrite	1	1.1	1e-9

Table 2 Electrical properties of human tissues

Material	Dielectric constant (permittivity) [C2/(N·m^2)]	Permeability [H/m]	Electric Conductivity [S/m]
Muscle	52.72	1	1.73
Fat	5.28	1	0.1
Skin	38	1	1.46

Table 3 Electrical properties of rat tissues.

Material	Dielectric constant (permittivity) [C2/(N·m^2)]	Permeability [H/m]	Electric Conductivity [S/m]
Muscle	45	1	1.5
Fat	10.56	1	1.4
Skin	29	1	1.5

Table 4 Tissue specific heat.

Tissue	Specific heat [J kg/m^3]
Muscle	3790
Fat	2300
Skin	2570

IV. Numerical Results

Significant variations in the scattering parameters were observed in the simulations due to the presence of insulating material and biological tissues, along with changes in the SAR values within these tissues. These findings give important suggestion about clinical applicability of implantable devices.

The presence of a PDMS coating notably affects S11 and S22 values. The system simulated in free space, without coating, exhibited lower scattering parameters (Fig. 4), indicating better performance compared to the encapsulated configurations. A slight improvement in both parameters was observed as PDMS thickness increased, highlighting the importance of considering both material type and layer thickness in antenna design.

As shown in Fig. 5, the scattering parameters tend to improve when biological tissues are introduced in the model. These simulations included a 2 mm PDMS coating and considered the presence or absence of a fibrotic capsule. The fibrotic layer introduces an additional interface, increasing wave reflections and thus degrading the scattering parameters, except for S22 in cases with low BMI. However, this variation remains limited (below 2%). BMI differences did not significantly affect scattering values, indicating minimal influence of body composition on reflection behavior.

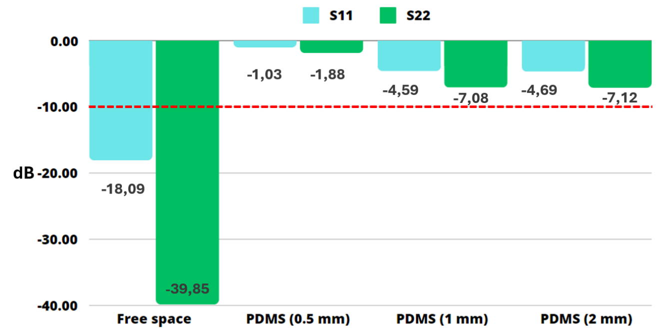

Figure 4 Scattering parameters S11 and S22 as a function of different PDMS thickness values.

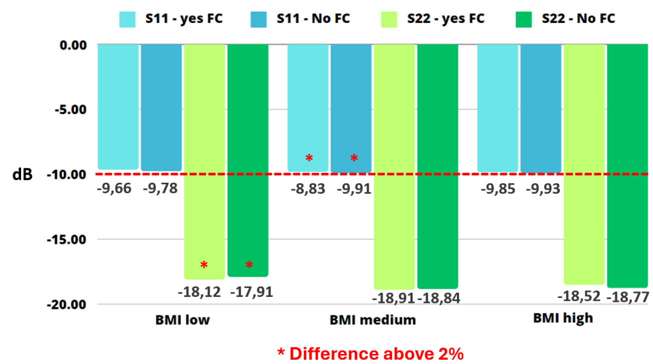

Figure 5 S11 and S22 scattering parameters with different BMI.

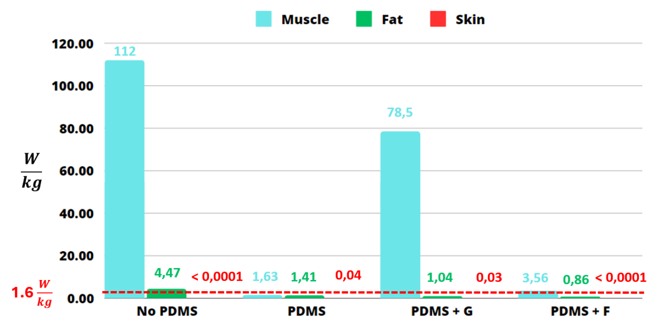

Figure 6 SAR with different coatings, G graphene and F ferrite both added to the PDMS.

Regarding SAR, Fig. 6 shows that the highest absorption levels occur in the absence of encapsulation or when using the graphene-enhanced PDMS coating. While the nanocomposite improves scattering parameters, it leads to a significant SAR increase compared to PDMS alone. To address this, the graphene layer was replaced with ferrite inside COMSOL simulation, a material reported in the literature for reducing SAR in implantable antennas.

BMI-related effects on SAR were also assessed (Fig. 7). Muscle tissue consistently exhibited the highest SAR values due

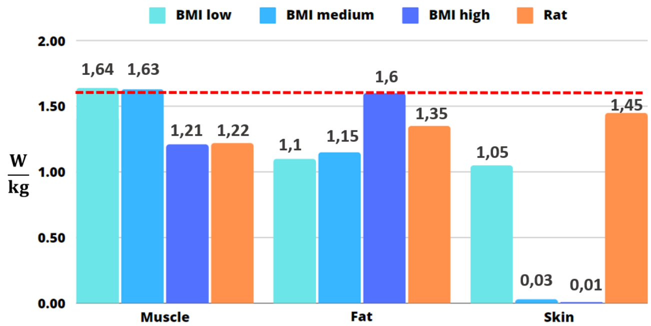

Figure 7 SAR with different BMI and rat tissue.

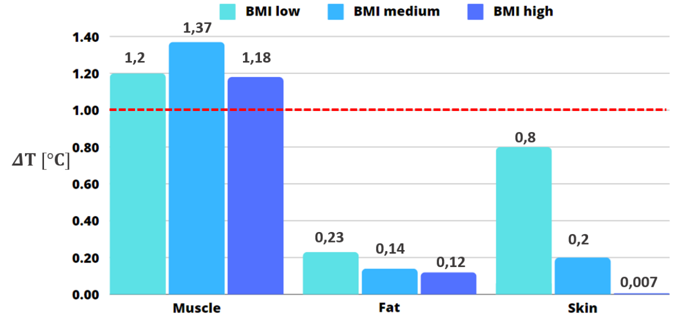

Figure 8 Temperature in human tissues with different BMI.

due to its higher conductivity. A clear trend emerged: SAR increases with the thickness of muscle and skin layers but decreases with increasing fat tissue. This underscores the need to balance transmission efficiency with safety requirements, an essential aspect for regulatory approval of medical devices, as emphasized in Regulation 2017/745.

Finally, a parallel model was developed to evaluate the behavior of the device in a preclinical scenario. The aim is to assess whether such simulations can reduce the extent of animal experimentation required during the early stages of device research. A final simulation was performed using a rat tissue model (Fig. 7), with a PDMS layer thickness of 2 mm. Compared to the human models, SAR values differed across tissues due to electrical property mismatches. Rat fat, with higher conductivity (1.5 S/m versus 0.1 S/m in humans), absorbed more radiation. As a result, SAR in rat adipose tissue was higher than in the human low-BMI case, despite matching thickness. Similar deviations were seen in skin and muscle layers, indicating that the animal model may not fully predict human outcomes due to these interspecies differences.

To complete the analysis temperature studies (Fig. 8) were conducted on human simulations with different BMI. In the muscle, the simulated PIFA antenna caused a temperature increase exceeding the 1°C regulatory threshold across all BMI groups. This is directly linked to electromagnetic absorption, as thermal rise corresponds with SAR levels. Interestingly, temperature in the medium BMI case was slightly higher than in the low BMI model (within 2% variation), likely due to reduced fat insulation and increased outward heat dissipation. In contrast, high BMI configurations showed lower temperature increases, as the thicker fat layer dispersed heat more effectively, thus mirroring the SAR trend.

Compared to communication methods like ultrasonic telemetry or galvanic coupling, which suffer from attenuation or bandwidth limitations, the RF-based approach studied here offers a more favorable balance between miniaturization, energy efficiency, and data throughput, making it particularly suitable for continuous clinical monitoring applications.

V. Conclusion

We examined the performance of an implantable antenna in the presence of insulating materials and biological tissues, focusing on the scattering parameters and SAR values in the tissues. Our objective was twofold: to adopt a personalized approach for each patient, considering a wide range of BMI indices, and to introduce a temporal evaluation of the implant, integrating the fibrotic capsule into our analysis protocols. We also created a simulation to evaluate parallelism with a rat animal model.

Antenna performance analysis showed significant variations in scattering parameters and SAR values across tissues, affecting the clinical viability of implantable devices. PDMS coating notably influences S11 and S22 values. Uncoated configurations yield lower and more optimal readings, while increased PDMS thickness slightly improves performance. Biological tissues enhance scattering parameters, while fibrotic capsules cause minor degradation (<2%). SAR analysis using a human model (average BMI, 2 mm PDMS) showed high SAR levels in muscle without coating. PDMS reduces SAR, improving patient safety. Conversely, conductive materials like graphene raise SAR despite better transmission. Thus, design must balance efficiency and safety.

Comparisons with animal models across BMIs show differing results, questioning their predictive accuracy for humans. Overall, the study underscores the need to consider insulating layers, tissue types, and fibrosis when designing implantable antennas to meet safety standards. The antenna's 2.4 GHz frequency aligns with BLE technology, enabling relevant performance benchmarking. Our findings highlight the value of personalized design, accounting for material, biological, and geometric factors—especially in PIFA antennas, preferred for subcutaneous use due to their size-efficiency tradeoff.

The results presented in this study are specific to the PIFA antenna. Future work will explore alternative antenna types to generalize the conclusions and further optimize the communication link. The originality of this work lies in the combined evaluation of coating material effects, inter-patient variability through BMI modeling, long-term implant behavior with fibrotic capsule integration, and cross-species predictivity through rat models. To our knowledge, this represents a novel, multi-perspective simulation framework for evaluating subcutaneous implant communication performance and safety. These findings help improve the safety and effectiveness of implantable medical technologies, paving the way for future innovations in this field. Future steps may involve validating simulation results *ex vivo* and *in vivo*, considering metabolic consumption in animal models.

VI. Bibliografy

[1] M. Wilcox, H. Gregory, R. Powell, T. J. Quick, J. B. Phillips, "Strategies for peripheral nerve repair," *Current tissue microenvironment reports*, 1, 49-59, 2020.

[2] G. Hussain *et al.*, "Current status of therapeutic approaches against peripheral nerve injuries: a detailed story from injury to recovery." International journal of biological sciences 16.1 (2020): 116.

[3] A. Coviello, F. Linsalata, U. Spagnolini, M. Magarini, “Artificial neural networks-based real-time classification of eng signals for implanted nerve interfaces,” in IEEE Journal on Selected Areas in Communications, vol. 42, no. 8, pp. 2080-2095, Aug. 2024

[4] M. Khabiri, "Design and simulation of implantable PIFA in presence of ANSYS human body model for biomedical telemetry using ANSYS HFSS." *Ozen Engineering Inc* (2015).

[5] M. Bahrouni *et al.*, "Modeling of a compact, implantable, dual-band antenna for biomedical applications." *Electronics* 12.6 (2023): 1475.

[6] J. Zhang *et al.*, "A compact dual-band implantable antenna for wireless biotelemetry in arteriovenous grafts." *IEEE Transactions on Antennas and Propagation* 71.6 (2023): 4759-4771.

[7] M. Sang *et al.*, "Ultra-thin flexible encapsulating materials for soft bio-integrated electronics." Advanced Science 9.30 (2022): 2202980.

[8] M. Mariello *et al.*, "Recent advances in encapsulation of flexible bioelectronic implants: Materials, technologies, and characterization methods." Advanced Materials 34.34 (2022): 2201129

[9] A. Carnicer-Lombarte *et al.*, "Foreign body reaction to implanted biomaterials and its impact in nerve neuroprosthetics." Frontiers in Bioengineering and Biotechnology 9 (2021): 622524.

[10] A. Béraud *et al.*, “Graphene field-effect transistors as bioanalytical sensors: Design, operation and performance,” *Analyst* 146.2 (2021): 403-428.

[11] C. Quartana *et al.*, "Wireless data transfer for Implanted Real-time Peripheral Nerve Interfaces." *EAI International Conference on Body Area Networks*. Cham: Springer Nature Switzerland, 2024.

[12] A. Coviello *et al.*, "Spike-Based High-Efficiency Data Compression Method for Intra-Body Galvanic Communication in Implantable Devices." *EAI BODYNETS,* 2024, pp. 1-17.

[13] S. Sukhija, and S. Rakesh Kumar, "A U-shaped meandered slot antenna for biomedical applications," in *Progress in Electromagnetics Research M* 62 (2017): 65-77.

[14] J. Abadia *et al.*, "3D-spiral small antenna design and realization for biomedical telemetry in the MICS band," *Radioengineering* 18.4 (2009): 359-367.

[15] H. T. Chattha *et al.*, "Compact Low-Profile DualPort Single Wideband Planar Inverted-F MIMO Antenna," in *IEEE Antennas and Wireless Propagation Letters*, 2013, 12: 1673-1675.

[16] M. M. Khan, H. Tabia, "Compact planar inverted F antenna (PIFA) for smart wireless body sensors networks," in *Engineering Proceedings*, 2.1 2020.

[17] M.M. Soliman *et al.*, "Review on medical implantable antenna technology and imminent research challenges." Sensors 21.9 (2021): 3163.

[18] N. A. Malik *et al.*, "Implantable antennas for bio-medical applications." in *IEEE Journal of Electromagnetics, RF and Microwaves in Medicine and Biology* 5.1 (2020): 84-96.

[19] “Comsol multiphysics.” [Online]. Available: https://www.comsol.it

[20] M. S. Islam *et al.*, "A serpentine PIFA antenna for implantable RFID tag," in Proc. *International Symposium on Antennas and Propagation (ISAP)*, Hobart, TAS, Australia, 2015

[21] K. M. Jeong *et al.*, "Ultrasonographic analysis of facial skin thickness in relation to age, site, sex, and body mass index," in *Skin Research and Technology*, 29.8, 2023.

[22] T. Abe, J. P. Loenneke, T. Fukunaga, "Interrelationships between body mass to waist circumference ratio, body mass index, and total body muscularity in older women," im *Journal of Clinical Gerontology and Geriatrics*, 5.2 (2014): 58-60.

[23] B. Nadeem, B. Raham, S. A. Gilani, "Correlation of subcutaneous fat measured on ultrasound with body mass index," in *Journal of medical ultrasound*, 26.4 (2018): 205-209.

[24] F. Caspers, "RF engineering basic concepts: S-parameters." arXiv preprint arXiv:1201.2346 (2012).

[25] I. Williams *et al.*, "SenseBack–Implant considerations for an implantable neural stimulation and recording device," in Proc. 2019 IEEE Biomedical Circuits and Systems Conference (BioCAS). IEEE, 2019.